



國立中山大學 通訊工程研究所

碩士論文

Institute of Communications Engineering

National Sun Yat-sen University

Master Thesis

資料相關性疊加訓練系統中無資料辨別問題之完美序

列預編碼架構

A Precoding Scheme Based on Perfect Sequences without Data

Identification Problem for Data-Dependent Superimposed

Training

研究生：林育星

Yu-Sing Lin

指導教授：李志鵬 博士

Dr. Chih-Peng Li

中華民國 100 年 7 月

July 2011

國立中山大學研究生學位論文審定書

本校通訊工程研究所碩士班

研究生林育星（學號：983070008）所提論文

資料相關性疊加訓練系統中無資料辨別問題之完美序列預編
碼架構

A Precoding Scheme Based on Perfect Sequences without Data
Identification Problem for Data-Dependent Superimposed
Training

於中華民國 100 年 7 月 25 日經本委員會審查並舉行口試，符
合碩士學位論文標準。

學位考試委員簽章：

召集人	<u>李育星</u>	委員	<u>王治良</u>
委員	<u>溫志宏</u>	委員	<u>鍾嘉聰</u>
委員	_____	委員	_____
委員	_____	委員	_____

指導教授李志鵬

李志鵬

誌謝

兩年的碩班生涯已到了尾聲，首先我要感謝父母與家人，他們在我人生旅途中遇到疑惑時能適時的給予意見與鼓勵，全力支持我，讓我無後顧之憂的完成論文。再來我要感謝指導教授李志鵬博士，老師不僅在我的研究上提供寶貴的意見與嚴格的訓練，更利用課餘時間不時給予正確的人生態度與職場生態概況，讓我有積極的心態面對未來。

另外要感謝博士班的貴程學長在我的研究上不厭其煩的給予指導與協助，加強我不夠紮實的部份，讓我的研究內容更加充實與完善。中山無線資訊傳輸系統實驗室是一個具有專業通訊領域與充滿歡笑的實驗室，是少數軟硬體如此充足的實驗室，我在這兩年裡得到許多專業與回憶，謝謝各位學長姊、同學以及學弟妹們的配合與幫助，為我碩班生涯劃下美麗的句點。最後，我要感謝口試委員：王晉良教授、溫志宏教授、鐘嘉德教授與蘇育德教授，不吝於對本論文給予指導與建議，在此由衷的感謝各位教授的指導。

林育星 謹誌

2011.07 于西灣



中文摘要

通道估測在接收端是一個相當重要的環節，領航訊號以等間隔方式安插於傳送資料之中將會得到最小通道均方差。傳統分時多工的方法是將資料與領航訊號以不同的時間點傳送，此方法會降低頻寬使用效率；另一方法是將訓練序列與資料直接疊加之後再傳送，但此估測的效果不佳。當使用資料相關性疊加訓練技術時，不僅保留了頻寬效益且估測的通道頻率響應精準度與分時多工技術一樣，但由於資料在傳送之前必須移除資料的循環平均值，而接收端在不知道此循環平均值的情況下無法有效的將訊號還原，如果利用較高的調變技術，接收端發生誤判的機率更加嚴重，錯誤率高居不下。

本論文中，我們利用奇異值分解分析發生誤判的主要原因並且使用預編碼技術解決此問題，根據分析的結果列出幾項有利於預編碼矩陣提升系統效能的條件，並且提出一個同時滿足這些條件的預編碼矩陣。此矩陣是由一反離散傅立葉轉換矩陣與一對角元素為完美序列的對角矩陣所構成。最後，利用電腦模擬驗證我們的方法是可行的，由錯誤率效能圖得知資料誤判的問題已藉由提出的方法解決。

關鍵字—分時多工、資料相關性疊加訓練技術、奇異值分解、反離散傅立葉轉換矩陣、完美序列。

Abstract

In data-dependent superimposed training (DDST) system, the data sequence subtracts a data-dependent sequence before transmission. The receiver cannot correctly find the unknown term which causes an error floor at high SNR.

In this thesis, we list some helpful conditions to enhance the performance for precoding design in DDST system, and analyze the major cause of data misidentification by singular value decomposition (SVD) method. Finally, we propose a precoding matrix based on [C.-P. Li and W.-C. Huang, “A constructive representation for the Fourier dual of the Zadoff–Chu sequences,” *IEEE Trans. Inf. Theory*, vol. 53, no. 11, pp. 4221–4224, Nov. 2007]. The precoding matrix is constructed by an inverse discrete Fourier transform (IDFT) matrix and a diagonal matrix with the elements consist of an arbitrary perfect sequence. The proposed method satisfies these conditions and simulation results show that the data identification problem is solved.

Keywords — Data-dependent superimposed training (DDST), inverse discrete Fourier transform (IDFT), singular value decomposition (SVD), Zadoff–Chu sequences.

Contents

論文審定書	i
誌謝	ii
中文摘要	iii
Abstract	iv
Chapter 1 Introduction	1
Chapter 2 System Model	5
2.1 Traditional SC-FDE System	5
2.2 DDST System	6
Chapter 3 Previous Literatures	12
3.1 Iterative Symbol-by-Symbol Detection Algorithm	12
3.2 Infinite Constellation Shift Algorithm	13
3.3 Gradient Infinite Constellation Shift Algorithm	17
Chapter 4 Proposed Method	19
4.1 Condition Description	19
4.2 Real or Complex Precoding Matrix	27
4.3 Proposed Precoding Matrix	30
Chapter 5 Simulation Results	32
Chapter 6 Conclusion and Future Works	37

6.1 Conclusions	37
6.2 Future Works	38
References.....	39
Abbreviations.....	44

List of Figures

Fig. 2.1.	The transmitter and receiver structure of SC-FDE.	6
Fig. 2.2.	The training sequence and the distortion data block are represented in time domain and frequency domain.	9
Fig. 3.1.	An ISSD scheme for DDST system.	13
Fig. 3.2.	First hard decision for finite constellation.....	14
Fig. 3.3.	A process diagrams for ICS algorithm. The circles represent the symbols location.	16
Fig. 3.4.	The relationship between $\alpha_{i,j}$ and IDFT matrix.	18
Fig. 4.1.	Propose structure based on DDST system.	20
Fig. 5.1.	PAPR Performance of different schemes (QPSK, $N=64$, $L=16$).	34
Fig. 5.2.	PAPR Performance of different schemes (QPSK, $N=64$, $L=8$).	34
Fig. 5.3.	Performance comparison of different schemes (BPSK, $N=64$, $L=4$).	35
Fig. 5.4.	Performance comparison of different schemes (BPSK, $N=64$, $L=8$).	35
Fig. 5.5.	Performance comparison of different schemes (QPSK, $N=256$, $L=32$).	36
Fig. 5.6.	Performance comparison of different schemes (QPSK, $N=64$, $L=8$).	36

List of Tables

Table I Compare Bandwidth Efficiency and Performance between Different Schemes..	9
Table II Common Matrices	31

Chapter 1 Introduction

Next generation wireless communication system must require excellent transmission speed and has ability to combat multipath effect. Family of multi-carrier schemes, such as orthogonal frequency division modulation (OFDM) system that is divided the available spectrum into a lot of flat fading subchannels and overlapping to enhance spectral efficiency. OFDM scheme has been employed in many transmission techniques such as worldwide interoperability for microwave access (WiMAX) [1], power line communication (PLC) [2], and the 3rd Generation Partnership Project (3GPP) Long Term Evolution (LTE) or other communications protocols. Compare to single carrier with frequency domain equalization (SC-FDE) transmission, there are main differences in system structure and system performance. For example, in OFDM systems, the transmission symbols are through an IDFT operation before transmission, this operation leads to generate peak-to-average power ratio (PAPR) in time domain [3], whereas SC-FDE has lower PAPR. In addition, the latter has full frequency diversity because the symbol energy is distributed to the available frequency band [4]. For these reasons, the PAPR and the bit error rate (BER) performance in SC-FDE systems is significantly better tolerability than uncoded OFDM systems.

Due to wireless communication suffers from severe interference caused by

frequency-selective fading channel. In order to avoid this problem, transmitter usually employs cyclic prefix (CP) technique, it not only mitigates multipath effect but also the received symbols can seem as circular convolution of the channel and data symbols [5]-[6], utilizing this property for reduce receiver complexity of channel equalization in frequency domain.

In high speed mobile communication environment, channel estimation is an important task at the receiver, the accuracy of channel estimation significantly affects system performance and the receiver complexity. In conventional superimposed training (ST) scheme, the channel state information (CSI) is estimated by using training sequence, which is known at the receiver and added to data symbols directly before transmission. However, the extra interference destroys the accuracy of channel estimation. In the time-division multiplexing (TDM) scheme, the pilot symbols and information symbols are separated transmission by different time slots. It leads to a bandwidth waste but the result of channel estimation is only affected by AWGN.

The pilot symbols are periodically inserted into transmitted data stream to obtain the minimum channel mean square error (MSE) [4], [7]. In order to save bandwidth, many researchers study in this issue for enhancing data rate [8]-[15], although these methods reserve bandwidth efficiency, the computational complexity of some of these methods are still high for channel estimation.

Precoded scheme is normally used to solve a lot of problems [4], [8]-[9], [12]-[13], [16]-[27], such as PAPR reduction [16], OFDM sidelobes discussion [17]-[18], interference cancellation problems [19]-[26], and power allocation [27]. In [8], a precoding scheme is proposed so-called DDST scheme, it not only achieves good estimation accuracy which is the same as TDM but also without loss of data rate, but it with some penalties in BER performance. In order to generate equal spaced pilot tones in frequency domain and achieve full data rate, the data symbols must subtract a distortion sequence (dependent on data symbols) which is unknown at the receiver. For some special cases, the distorted block will not correctly reconstruct at receiver, thereby, the BER performance is badly affected by distortion sequence. However, in [9], [29], two data detection methods have been proposed to search unknown value in the time and frequency domain, respectively. Their detection algorithms of high QAM modulation would reduce the probability of data misidentification, such that the BER performance could be improved, but the data identification problem still exists.

In this thesis, we find the leading cause of data misidentification by singular value decomposition (SVD) method [30]. According to the result of SVD analysis, we proposed a precoding matrix to solve this problem, and then listed some conditions that can help the precoding matrix to enhance system performance. The proposed matrix is constructed of a diagonal matrix and an IDFT matrix. The entries in the diagonal matrix

are a set of perfect sequence. Finally, the simulation results show that the proposed method is feasible. Since the data misidentification problem is solved, the BER performance is better than previous work.

This thesis is organized as follows. The DDST system model is described in Chapter 2. The data identification problem and previous researches are discussed in Chapter 3. In Chapter 4, we find the major reason of data misidentification and propose a precoding scheme for DDST system. Then, Chapter 5 displays the simulation results. Finally, the conclusions and future works are drawn in Section 6.

Chapter 2 System Model

2.1 Traditional SC-FDE System

We consider a SC-FDE transmission that the CP length is sufficient to prevent the inter-block-interference (IBI) and inter-symbol interference (ICI). Fig. 2.1 displays the structure of traditional SC-FDE. Let $\mathbf{h} = [h_0, h_1, h_2, \dots, h_{L-1}]^T$ denotes the channel impulse response and the block length is N . Assume the CP length is $V = L$ to save bandwidth efficiency and the multipath channel is time-invariant over a block. The i -th transmitted block can be expressed as

$$\mathbf{x}_i = [x_{i,0}, x_{i,1}, x_{i,2}, \dots, x_{i,N-1}]^T, \quad (2.1)$$

due to CP, the received block \mathbf{s}_i can be expressed as

$$\mathbf{s}_i = \mathbf{H}_i \mathbf{x}_i + \mathbf{n}_i, \quad (2.2)$$

where \mathbf{n}_i is $N \times 1$ independent additive white Gaussian noise (AWGN) with zero mean and variance σ_N^2 , and \mathbf{H} is an $N \times N$ circulant matrix which can be diagonalized by the discrete Fourier transform (DFT) matrix [4], [5], i.e., $\mathbf{H} = \mathbf{F}^H \mathbf{D} \mathbf{F}$. \mathbf{D} is a diagonal matrix whose entries on the diagonal elements are frequency response of the channel at each subcarriers.

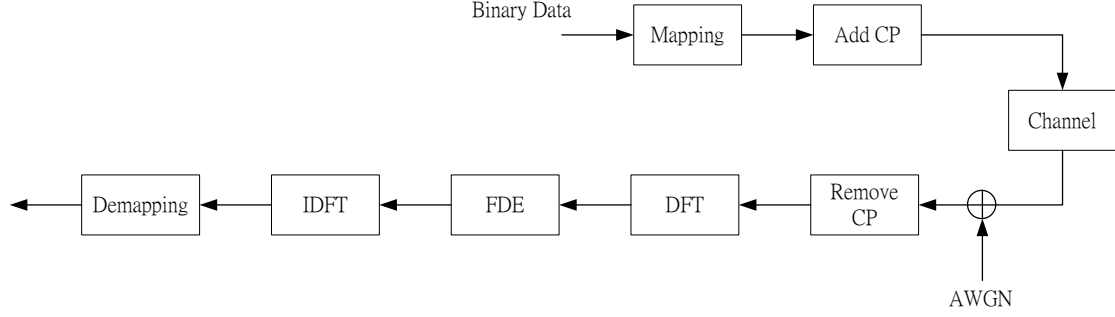


Fig. 2.1. The transmitter and receiver structure of SC-FDE.

2.2 DDST System

In precoded SC system, the precoding matrix direct mapping data block \mathbf{z}_i to \mathbf{x}_i before transformation, and it is well known that arranging pilot symbols equal spaced in frequency domain can obtain the best channel estimation performance by performing least square (LS) channel estimation [7]. We define the i -th transmitted block as

$$\mathbf{x}_i = \mathbf{P}\mathbf{z}_i + \mathbf{c}, \quad (2.3)$$

where \mathbf{P} is a $N \times N$ precoding matrix, and \mathbf{c}_i is the training sequence with size $N \times 1$. In DDST system, assume $Q = N/K$ is an integer and $K = L$, the precoding matrix \mathbf{P} can be expressed as

$$\mathbf{P} = (\mathbf{I} - \mathbf{J}), \quad (2.4)$$

where

$$\mathbf{J} = \mathbf{F}^H \mathbf{D}_p \mathbf{F} \quad (2.5)$$

and the diagonal matrix \mathbf{D}_p is given by

$$(\mathbf{D}_p)_{i,i} = \begin{cases} 1, & i \in \xi_p \\ 0, & \text{else,} \end{cases}$$

where $\xi_p = \{0, Q, 2Q, \dots, (K-1)Q\}$ is a set of pilot tone indexes. The matrix \mathbf{P} can be

rewritten as following equation

$$\mathbf{P} = (\mathbf{I} - \mathbf{J}) = \mathbf{F}^H \left\{ \begin{bmatrix} 1 & & & & \\ & 1 & & & \\ & & \ddots & & \\ & & & \ddots & \\ & & & & 1 \end{bmatrix} - \begin{bmatrix} 1 & & & & \\ & 0 & & & \\ & & \ddots & & \\ & & & 1 & \\ & & & & 0 \end{bmatrix} \right\} \mathbf{F}. \quad (2.6)$$

From Eq. 2.6, it is clear to see, the operation of matrix subtraction in the brace that is equivalent to remove the information symbols distributed on pilot subcarriers in frequency domain, and this operation can be translate to time domain performed by DFT matrix.

After matrix multiplication, matrix \mathbf{J} can be derived as

$$\mathbf{J} = \frac{1}{Q} \begin{bmatrix} \mathbf{I}_K & \cdots & \cdots & \mathbf{I}_K \\ \vdots & \ddots & & \vdots \\ \vdots & & \ddots & \vdots \\ \mathbf{I}_K & \cdots & \cdots & \mathbf{I}_K \end{bmatrix}_{KQ \times KQ}, \quad (2.7)$$

where \mathbf{J} is selecting equally spaced Q symbols from the data block, so we can divide a

data block into K subgroups. The cyclic mean of the data, μ_i , which is the mean of a subgroup, it can be define as

$$\mu_j = \frac{1}{Q} \sum_{m=0}^{Q-1} \mathbf{a}_i(j+mK), j = 0, 1, 2, \dots, K-1, \quad (2.8)$$

where \mathbf{a}_i as the i -th precoded block, i.e., $\mathbf{a}_i = (\mathbf{I} - \mathbf{J})\mathbf{z}_i$, and $\tilde{\mathbf{a}}_{i,j}$ as the j -th subgroup of \mathbf{a}_i , which can be expressed as

$$\tilde{\mathbf{a}}_{i,j} = [\mathbf{a}_i(j), \mathbf{a}_i(j+K), \dots, \mathbf{a}_i(j+(Q-1)K)]. \quad (2.9)$$

Each subgroup can be treated individually [9], [29]. In order to avoid enhancing PAPR, DDST system uses perfect sequences as training sequence. Perfect sequences have constant magnitude both in time and frequency domain, such as Zadoff-Chu sequence or chirp sequences. The sequence \mathbf{c} can be expressed as

$$c[n] = \begin{cases} e^{\frac{-j2\pi n^2}{K}}, & n = 0, 1, \dots, N-1, \text{ for even } K \\ e^{\frac{-j2\pi n(n+1)}{K}}, & n = 0, 1, \dots, N-1, \text{ for odd } K. \end{cases} \quad (2.10)$$

Since sequence \mathbf{c} is periodic and its period is K , using properties of the DFT, after the data-dependent sequence is added to pure information block, i.e., $\mathbf{z}_i - \mathbf{J}\mathbf{z}_i$, the frequency response of distortion block will appear nulls on these pilot subcarriers, and the pilot symbols will be regularly arranged at corresponding positions, it is shown in Fig. 2.2.

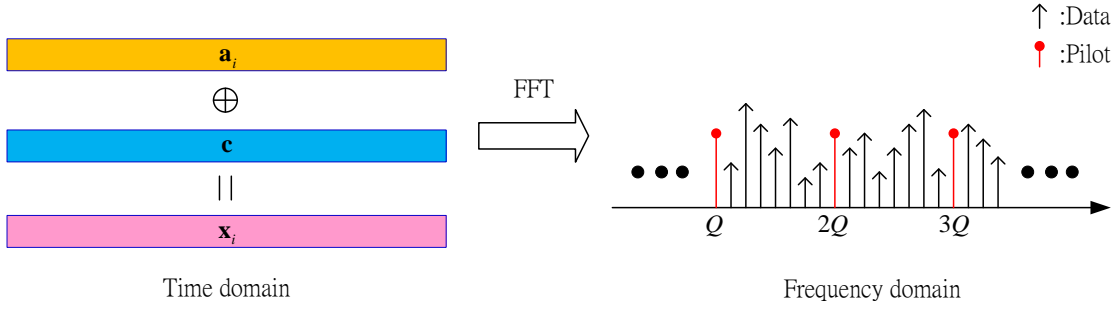


Fig. 2.2. The training sequence and the distortion data block are represented in time domain and frequency domain.

Table I

Compare Bandwidth Efficiency and Performance between Different Schemes

Scheme	Bandwidth efficiency	Channel estimation performance
Traditional ST	100%	Poor
TDM	$N/(N+L) \times 100\%$	Accuracy
DDST	100%	Same as TDM

DDST is a new pilot insertion scheme that can accommodate a good channel estimation quality and reserve bandwidth. For traditional ST scheme, its channel estimation error will be adding extra interference that from the data, which degrading the performance seriously. An alternative approach is TDM scheme, which decreases the bandwidth efficiency since one preamble block needs to be transmitted periodically. In Table II, the above mentioned schemes have been compared with DDST scheme.

At receiver, we assume synchronization are perfect, and the CSI is known at receiver. After channel estimation, the training sequence \mathbf{c} can be easily removed from \mathbf{s}_i by a simple operation

$$\mathbf{r}_i = (\mathbf{I} - \mathbf{J})\mathbf{s}_i. \quad (2.11)$$

It equivalent to clearing the DFT of \mathbf{s}_i at pilot tones in frequency domain, it can be rewritten as

$$\mathbf{r}_i = \mathbf{H}(\mathbf{I} - \mathbf{J})\mathbf{x}_i + \mathbf{n}_i. \quad (2.12)$$

Since \mathbf{H} is a circulant matrix such that channel equalization can be accomplished in frequency domain, it is shown as

$$\bar{\mathbf{r}}_i = \mathbf{F}^H \mathbf{W} \mathbf{F} \mathbf{r}_i, \quad (2.13)$$

where \mathbf{W} is a diagonal matrix and each element is

$$W(k) = \frac{1}{H_k} \quad (2.14)$$

and

$$W(k) = \frac{H_k^*}{|H_k|^2 + \sigma_N^2} \quad (2.15)$$

for zero-forcing (ZF) and minimum mean-square-error (MMSE) criterion respectively.

We define the superscript $*$ denotes the complex conjugate and H_k is frequency response of channel at k -th subcarrier. Note the ZF equalizer does not consider the effect of noise. It leads to system performance degradation due to noise enhancement

[31]. For this reason, we only consider the MMSE equalizer which provides balanced solution to suppress the effects of noise.

Note the precoding matrix $(\mathbf{I} - \mathbf{J})$ is a nonlinear transformation since it is not full rank [9]. Inverse of this precoding matrix is not existed such that the data is hard to detect at receiver. Some data detection methods have been proposed to solve this problem. In section III, we will introduce some detection methods and data identification problem in detail.

Chapter 3 Previous Literatures

3.1 Iterative Symbol-by-Symbol Detection Algorithm

In [8], iterative symbol-by-symbol detection (ISSD) algorithm was proposed, it shown in Fig. 3.1. So far, this detection algorithm has the lowest computation complexity for DDST system. The process can be summarized as follows

Step 1 Treating \mathbf{Jz}_i as an extra additive noise at first hard decision, the initial hard decision of $\bar{\mathbf{r}}_i$ is given by

$$\hat{\mathbf{r}}_i^{(0)} = \lfloor \bar{\mathbf{r}}_i \rfloor_{\mathcal{A}}, \quad (3.1)$$

where $\lfloor \mathbf{v} \rfloor_{\mathcal{A}}$ demotes the vector of constellation points that are closest to the vector \mathbf{v} and selected from finite alphabet, \mathcal{A} .

Step 2 The detected symbols are used to reconstruct \mathbf{Jz}_i to be compensated for distorted symbols which caused by data dependent sequence. The compensated symbols at l -th iteration are given by

$$\hat{\mathbf{r}}_i^{(l)} = \lfloor \bar{\mathbf{r}}_i + \mathbf{J}\hat{\mathbf{r}}_i^{(l-1)} \rfloor_{\mathcal{A}}. \quad (3.2)$$

The iterations will not stop until achieving the predefined number of iterations. When using small constellation sizes since the artificial distortion term \mathbf{Jz}_i can be seen as another noise term in low SNR. In high SNR, It has error floor due to the interference

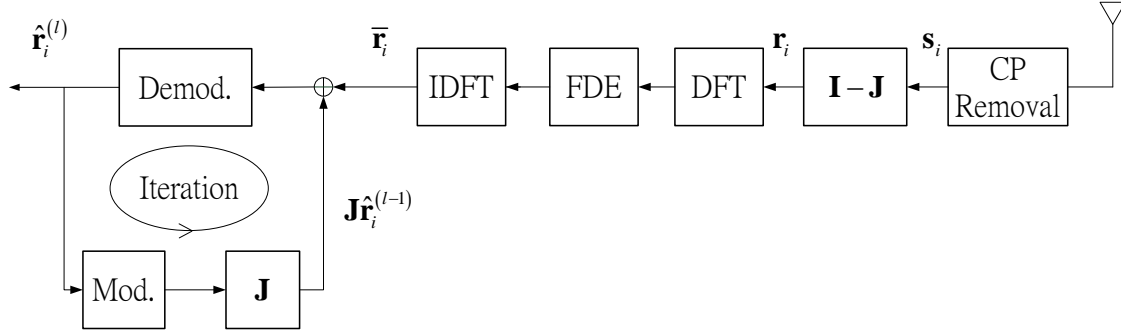


Fig. 3.1. An ISSD scheme for DDST system.

term. For long length subgroup, its average value is usually closed to zero such that the effect of artificial distortion is approximately equal to zero. So, ISSD algorithm can achieve good result with less interference for long length subgroup.

3.2 Infinite Constellation Shift Algorithm

For high-order QAM signals, ISSD has poor BER since the first hard decision is not reliable as shown in Fig. 3.2. Cyclic mean causes information data block a shift in constellation as Fig. 3.2 (b). The first hard decision would lose accuracy for some edge symbols even in noiseless environment as Fig. 3.2 (c). To support high data rate when high-order QAM constellations was employed in DDST system, infinite constellation shift (ICS) algorithm was proposed in [29]. Since the distorted subgroup shifted an unknown value on the constellation as shows in Fig. 3.2. (b), they should search a suitable value $\hat{\mu}$ which minimizes the following cost function

$$\hat{\mu} = \arg \min_{\hat{\mu}} \left\| \tilde{\mathbf{a}}_{i,j} + \hat{\mu} - \lfloor \tilde{\mathbf{a}}_{i,j} + \hat{\mu} \rfloor_{\mathcal{A}} \right\|_2. \quad (3.3)$$

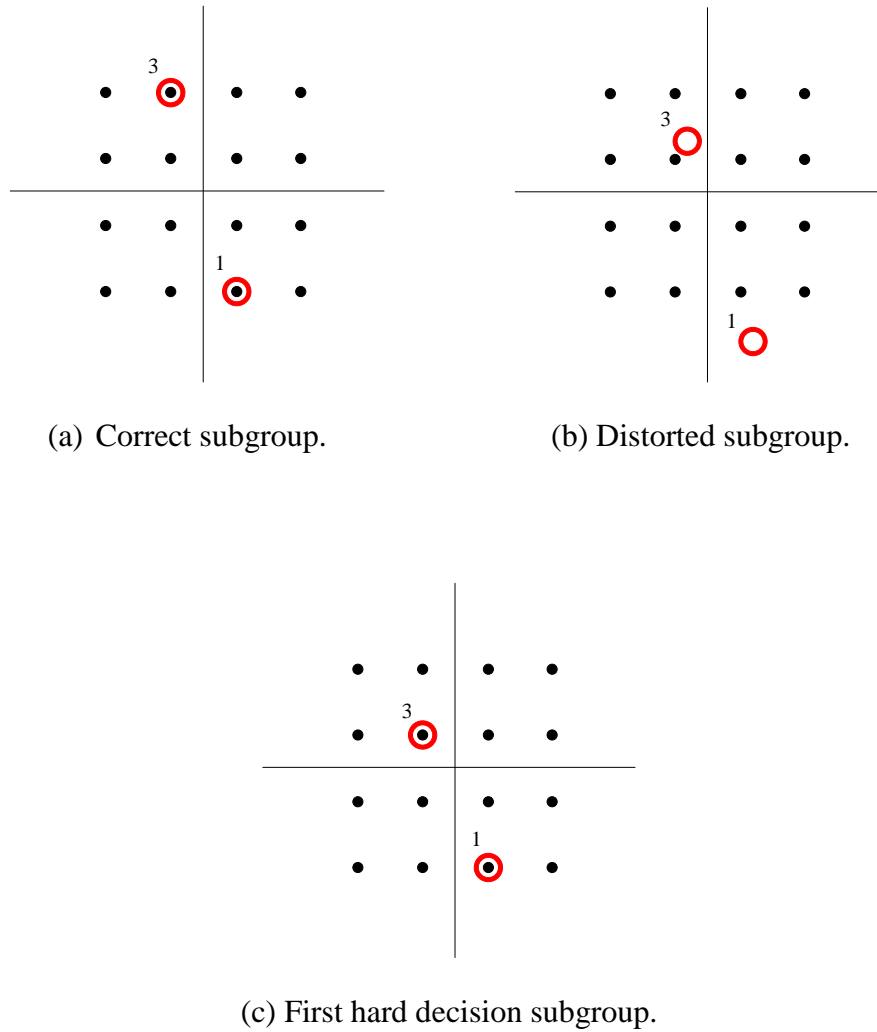


Fig. 3.2. First hard decision for finite constellation.

In order to maintain subgroup structurally, the best value of $\hat{\mu}$ can obtain by two step, a fine revision, $\hat{\mu}_{\text{small}}$, and a unit step revision, $\hat{\mu}_{\text{large}}$. The process can be summarized as following

Step 1 Building an infinite unit-spaced alphabet, \mathcal{A}_{∞} , and \mathcal{A} must satisfy the following

$$\mathcal{A} \subset \mathcal{A}_{\infty}. \tag{3.4}$$

Step 2 A best value of $\hat{\mu}_{\text{small}}$ is selected to minimize the cost function, it is given by

$$\hat{\mu}_{\text{small}} = \arg \min_{\hat{\mu}_{\text{small}}} \left\| \tilde{\mathbf{a}}_{i,j} + \hat{\mu}_{\text{small}} - \left\lfloor \tilde{\mathbf{a}}_{i,j} + \hat{\mu}_{\text{small}} \right\rfloor_{\mathcal{A}_\alpha} \right\|_2, \quad (3.5)$$

where $\hat{\mu}_{\text{small}} \in 0, 2\alpha, \dots, 1-\alpha$. It is a trade-off between search resolution and computation complexity for the value of α sets.

Step 3 A best value of $\hat{\mu}_{\text{large}}$ is selected to minimize the cost function, it is given by

$$\hat{\mu}_{\text{large}} = \arg \min_{\hat{\mu}_{\text{large}}} \left\| \tilde{\mathbf{a}}_{i,j} + \hat{\mu}_{\text{small}} + \hat{\mu}_{\text{large}} - \left\lfloor \tilde{\mathbf{a}}_{i,j} + \hat{\mu}_{\text{small}} + \hat{\mu}_{\text{large}} \right\rfloor_{\mathcal{A}} \right\|_2, \quad (3.6)$$

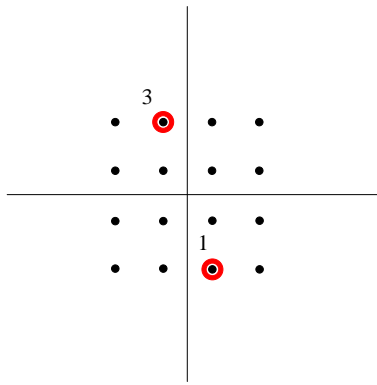
where $\hat{\mu}_{\text{large}} \in 0, \pm 1, \pm 2, \dots$. After both $\hat{\mu}_{\text{small}}$ and $\hat{\mu}_{\text{large}}$ are obtained, the best value of $\hat{\mu}$ can be expressed as

$$\hat{\mu}_{\text{best}} = \hat{\mu}_{\text{small}} + \hat{\mu}_{\text{large}}. \quad (3.7)$$

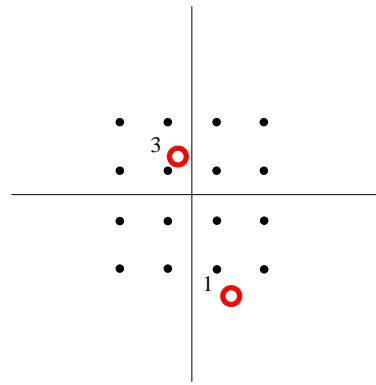
$\hat{\mu}_{\text{best}}$ is add to the distorted subgroup, and utilizes hard decision over a finite alphabet \mathcal{A} to get detection subgroup $\hat{\mathbf{a}}_{i,j}$. The process is illustrated in Fig.

3.3.

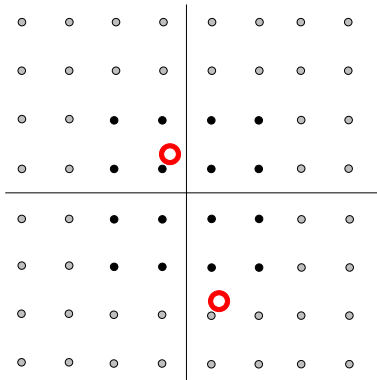
Notice that if the mean of non-distorted subgroup is zero, this operation is not necessary. Due to orthogonal constellation, the real and imaginary parts can be computed separately, it leads to a lower complexity. However, ICS algorithm is useless for QPSK or BPSK modulations. It is to be expected since mean of subgroup can never be more than a half distance of nearest constellation points. It causes to expand



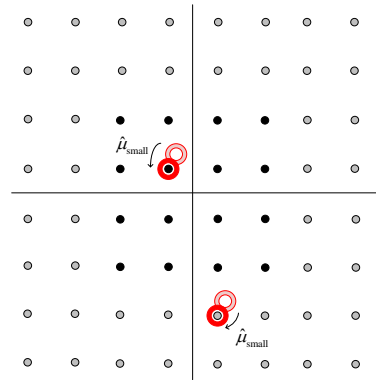
(a) Correct subgroup.



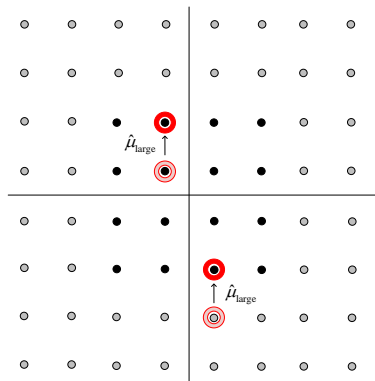
(b) Distorted subgroup.



(c) Extend the constellation.



(d) Search and add $\hat{\mu}_{\text{small}}$.



(e) Search and add $\hat{\mu}_{\text{large}}$.

Fig. 3.3. A process diagrams for ICS algorithm.

original constellation \mathcal{A} to infinite constellation \mathcal{A}_∞ did not work. ICS algorithm is the same to the first hard decision in ISSD for QPSK and BPSK modulations.

3.3 Gradient Infinite Constellation Shift Algorithm

In [9], gradient infinite constellation shift (GICS) algorithm was proposed. Note every subgroup $\tilde{\mathbf{a}}_{i,j}$ in frequency domain must have at least one null subcarrier. For this reason, the detection scheme uses gradient descent method to search for the loss information at null subcarrier of subgroup $\tilde{\mathbf{a}}_{i,j}$. The process can be summarized as following

Step 1 Building an infinite unit-spaced alphabet, \mathcal{A}_∞ , and \mathcal{A} must satisfy the following

$$\mathcal{A} \subset \mathcal{A}_\infty. \quad (3.8)$$

Step 2 Use a gradient descent method to fine the best value of $\alpha_{i,j}$ which is selected to minimize the cost function, it is given by

$$\left\| \tilde{\mathbf{a}}_{i,j} + \alpha_{i,j} \mathbf{f}_i - \left[\tilde{\mathbf{a}}_{i,j} + \alpha_{i,j} \mathbf{f}_i \right]_{\mathcal{A}_\infty} \right\|^2, \quad (3.9)$$

where \mathbf{f}_i is one of IDFT matrix column which corresponding to the null frequency index. Fig. 3.4 displays the relationship between $\alpha_{i,j}$ and IDFT matrix.

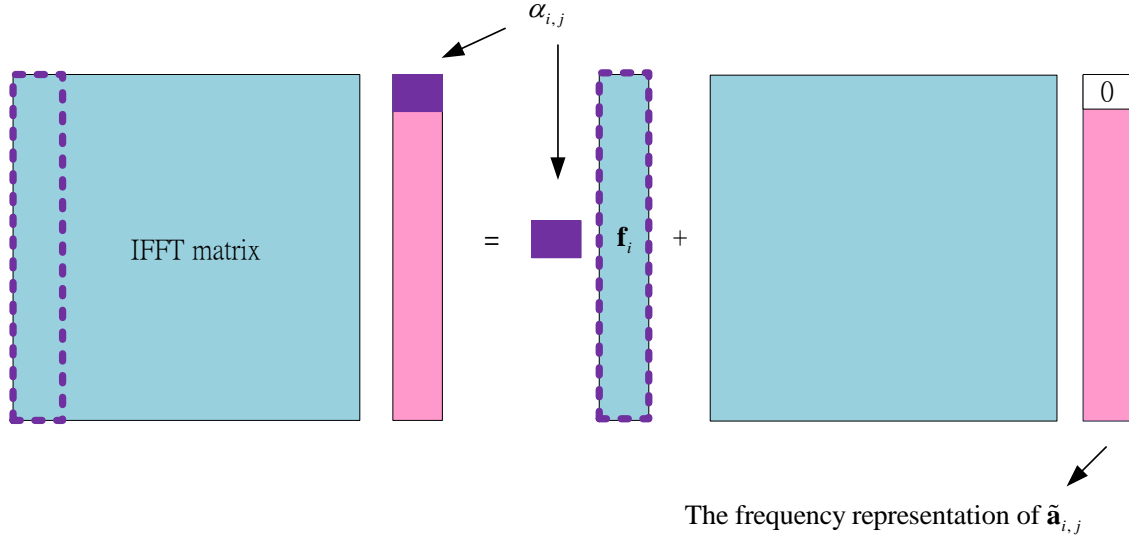


Fig. 3.4. The relationship between $\alpha_{i,j}$ and IDFT matrix.

Step 3 A best value of $\hat{\mu}'_{\text{large}}$ is selected to minimize the cost function, it is given by

$$\hat{\mu}'_{\text{large}} = \arg \min_{\hat{\mu}'_{\text{large}}} \left\| \tilde{\mathbf{a}}_{i,j} + (\alpha_{i,j} + \hat{\mu}'_{\text{large}}) \mathbf{f}_i - \left[\tilde{\mathbf{a}}_{i,j} + (\alpha_{i,j} + \hat{\mu}'_{\text{large}}) \mathbf{f}_i \right]_{\mathcal{A}} \right\|_2, \quad (3.10)$$

where $\hat{\mu}'_{\text{large}} \in 0, \pm 1, \pm 2, \dots$. After both $\alpha_{i,j}$ and $\hat{\mu}'_{\text{large}}$ are obtained, the sum of two parameters shall be compensated for loss information at null frequency of $\hat{\mathbf{a}}_{i,j}$.

GICS algorithm can be seen as ICS scheme implemented in frequency domain. It also splits the search for $\hat{\mu}_{\text{best}}$ into two parts. Using gradient algorithm to achieve a local optimal solution in frequency domain is similar to find $\hat{\mu}_{\text{small}}$ in time domain. For some special cases, more than one information data block has the same subgroup $\hat{\mathbf{a}}_{i,j}$. It is so called data identification problem [29]. It limited the performance improvement of the above researches. In order to enhance system performance, we propose a transceiver structure without data identification problem in next section.

Chapter 4 Proposed Method

As aforementioned, the data misidentification occurs when the modulation symbols of subblock is identical to each other and some special subgroups. Our aim is to prevent data misidentification and maintain the DDST system properties. A precoding matrix is adopted before transmission such that every transmitted subblock is unique as shown in Fig. 4.1. In this chapter, we illustrate essential conditions for a precoding matrix and propose an effective scheme.

4.1 Condition Description

Firstly, single carrier system has full frequency domain diversity [32]. It spreads energy of every data symbol to whole transmitted band and is robust to frequency selective fading channel. DDST system followed this characterization except on pilot subcarriers. The proposed precoding matrix should maintain this property, which is all columns must have equal gain in frequency domain. It leads to every data symbol is evenly extended to whole data transmitted band as in DDST system. Assume \mathbf{G} is a $N \times N$ precoding matrix, the ideal criterion is

$$\left| (\mathbf{F}\mathbf{G})_{n,m} \right| = \frac{1}{\sqrt{N}}, \quad 0 \leq n, m \leq N-1. \quad (4.1)$$

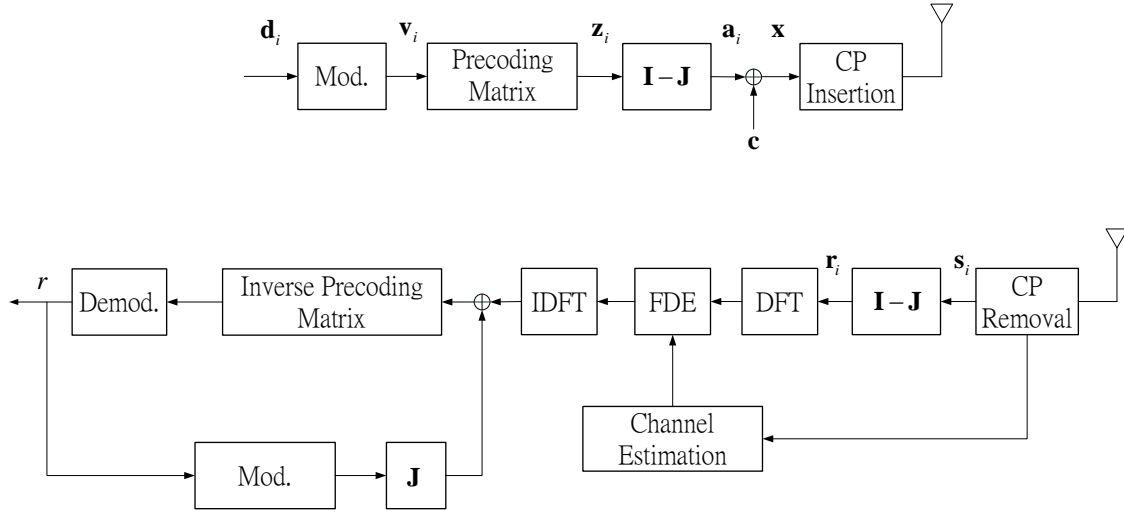


Fig. 4.1. Propose structure based on DDST system.

All columns of \mathbf{G} are given by

$$\mathbf{G} = [\mathbf{g}_0 \ \mathbf{g}_1 \ \mathbf{g}_2 \ \cdots \ \mathbf{g}_{N-1}]. \quad (4.2)$$

According to Wiener-Khinchin theorem, the relation of autocorrelation function and power spectrum density is shown as

$$R(\tau) = \int S(f) e^{j2\pi f\tau} df. \quad (4.3)$$

Equal Amplitude in frequency domain leads to autocorrelation in time domain is an impulse function. The autocorrelation of each column can be shown as

$$(C1) \quad R_{\mathbf{g}_m \mathbf{g}_m}(\tau) = \begin{cases} \text{constant}, & \tau = 0, \quad m = 1, 2, \dots, N \\ 0, & \tau \neq 0, \quad m = 1, 2, \dots, N, \end{cases} \quad (4.4)$$

where $R_{\mathbf{g}_m \mathbf{g}_m}(\tau)$ is defined by

$$R_{\mathbf{g}_m \mathbf{g}_m}(\tau) = \sum_{n=0}^{N-1} \mathbf{g}_m[n] \mathbf{g}_m^*[n+\tau]. \quad (4.5)$$

After multiplying matrix $(\mathbf{I} - \mathbf{J})$, each data symbols can spread energy to whole transmitted band except pilot subcarriers as in DDST system.

Secondly, data block can be separated into K subgroups and be detected independently at receiver in DDST system. For precoding matrix \mathbf{G} , information block \mathbf{z}_i can be expressed as

$$\mathbf{z}_i = \mathbf{G} \mathbf{b}_i, \quad (4.6)$$

where \mathbf{b}_i is the original data block. Note in DDST system information block \mathbf{z}_i is equal to original data block \mathbf{b}_i . In proposed scheme, the precoded data block \mathbf{a}_i should be shown as

$$\mathbf{a}_i = (\mathbf{P}_{\text{DDST}} \otimes \mathbf{I}_K) \mathbf{G} \mathbf{b}_i. \quad (4.7)$$

Matrix $(\mathbf{P}_{\text{DDST}} \otimes \mathbf{I}_K) \mathbf{G}$ should separate \mathbf{a}_i and \mathbf{b}_i into K independent subgroups. For precoding matrix \mathbf{G} , subgroups can be separated independently if the precoding matrix just moved the N/L elements into the same subgroup. It can be represented as

$$\mathbf{G} = \mathbf{E} \otimes \mathbf{I}_K, \quad (4.8)$$

where \mathbf{E} is a $Q \times Q$ matrix and can be seen as a principal submatrix. The equivalent

precoding matrix $(\mathbf{P}_{\text{DDST}} \otimes \mathbf{I}_K) \mathbf{G}$ can be shown as

$$(\mathbf{P}_{\text{DDST}} \otimes \mathbf{I}_K)(\mathbf{E} \otimes \mathbf{I}_K) = (\mathbf{P}_{\text{DDST}} \mathbf{E} \otimes \mathbf{I}_K). \quad (4.9)$$

It also keeps subgroups individual. The m th column of precoding matrix \mathbf{G} should be

$$(C2) \quad |g_m(n)| = 0, \text{ for } (n \bmod L) \neq (m \bmod L). \quad (4.10)$$

Under this condition, we can extend a small size matrix to the main matrix. To separate information data block into K subgroups not only reduce the complexity at receiver but also at transmitter when precoding.

Moreover, the inverse of precoding matrix is necessary in data detection at receiver.

Precoding matrix \mathbf{G} should be a unitary matrix. It can be shown as

$$\mathbf{G}^H \mathbf{G} = \mathbf{G} \mathbf{G}^H = \mathbf{I}, \mathbf{G}^{-1} = \mathbf{G}^H. \quad (4.11)$$

It is easy to prove the above equation is equivalent to

$$(C3) \quad \mathbf{E}^H \mathbf{E} = \mathbf{E} \mathbf{E}^H = \mathbf{I}, \mathbf{E}^{-1} = \mathbf{E}^H. \quad (4.12)$$

Next, we consider the data identification problem. We review the SVD method at first, and show how to utilize this tool to explain precoded subblock is uniquely determined.

The SVD method is a famous analysis tool for signal processing. A $p \times q$ matrix

\mathbf{A} can be decomposed uniquely as

$$\mathbf{A} = \mathbf{U}\mathbf{\Sigma}\mathbf{V}^H, \quad (4.13)$$

where $\mathbf{\Sigma}$ is a $p \times q$ matrix that diagonal elements of $\mathbf{\Sigma}$ are singular values of \mathbf{A} and

\mathbf{U} is an $p \times p$ orthonormal matrix. All column vectors of \mathbf{U} are the left singular

vectors of \mathbf{A} . Similarly, \mathbf{V} is an $q \times q$ orthonormal matrix, whose column vectors are

the right singular vectors of \mathbf{A} . The matrices are represented as follows

$$\mathbf{\Sigma}_{p \times q} = \begin{bmatrix} \sigma_0 & & & \\ & \sigma_1 & & \\ & & \ddots & \\ & & & \end{bmatrix}_{p \times q}, \quad (4.14)$$

$$\mathbf{U}_{p \times p} = [\mathbf{u}_0 \ \mathbf{u}_1 \ \cdots \ \mathbf{u}_{p-2} \ \mathbf{u}_{p-1}], \quad (4.15)$$

$$\mathbf{V}_{q \times q} = [\mathbf{v}_0 \ \mathbf{v}_1 \ \cdots \ \mathbf{v}_{q-2} \ \mathbf{v}_{q-1}]. \quad (4.16)$$

Consequently, every matrix can be factorized by two orthonormal matrices, we list three

important properties as below

(P1) Rank of \mathbf{A} , which is assumed to be k , is equal to the number of nonzero singular values of \mathbf{A} .

(P2) The first k left singular vectors $\mathbf{u}_0, \dots, \mathbf{u}_{k-1}$ from an orthonormal basis for range space of \mathbf{A} , i.e., $\mathbf{R}(\mathbf{A})$.

(P3) The last $q-k$ right singular vectors $\mathbf{v}_k, \dots, \mathbf{v}_{q-1}$ from an orthonormal basis for null space of \mathbf{A} , i.e., $\mathbf{N}(\mathbf{A})$.

From a linear algebra viewpoint, the precoding procedure just likes mapping operation. As mentioned in the previous chapter, matrix \mathbf{P}_{DDST} is a nonlinear transformation. If information symbol of the subblock is identical to each other, the receiver would confuse what signal is transmitted. We use SVD method to analyze this effect and expect every precoded subblock to be uniquely determined. It can be represented in mathematical as below

$$\Theta \tilde{\mathbf{z}}_{i,x} \neq \Theta \tilde{\mathbf{z}}_{i,y}, \quad (4.17)$$

where $\tilde{\mathbf{z}}_{i,x}, \tilde{\mathbf{z}}_{i,y} \in \Omega_{\text{ML}}$, $x \neq y$, and Ω_{ML} is a set of all possible transmit subgroups, which requires M^Q subgroups. M is modulation order, and Θ is a new precoding matrix, given by

$$\Theta = \mathbf{P}_{\text{DDST}} \mathbf{E}, \quad (4.18)$$

We rewrite Eq. (4.17) as follows

$$\Theta (\tilde{\mathbf{z}}_{i,x} - \tilde{\mathbf{z}}_{i,y}) \neq \mathbf{0}, \quad (4.19)$$

where $\mathbf{0}$ is a zero vector. Define $\tilde{\mathbf{z}}'_{i,k} = \tilde{\mathbf{z}}_{i,x} - \tilde{\mathbf{z}}_{i,y}$, it can be rewritten as

$$\Theta \mathbf{z}'_{i,k} \neq \mathbf{0}. \quad (4.20)$$

The above equation is impact

$$\mathbf{z}'_{i,k} \notin \mathbf{N}(\Theta), \quad (4.21)$$

i.e., any difference between arbitrary two information subgroups $\mathbf{z}'_{i,k}$ should not be combined by basis of the null space of Θ .

To use this tool in our discussion case, matrix \mathbf{P}_{DDST} is decomposed by SVD method as

$$\begin{aligned} \mathbf{P}_{\text{DDST}} &= \mathbf{U}_D \Sigma_D \mathbf{V}_D^H \\ &= [\mathbf{u}_0^D, \dots, \mathbf{u}_{Q-1}^D] \begin{bmatrix} \dot{\sigma}_{0,0}^D & & & \\ & \ddots & & \\ & & \dot{\sigma}_{Q-2,Q-2}^D & \\ & & & 0 \end{bmatrix} [\mathbf{v}_0^D, \dots, \mathbf{v}_{Q-1}^D]^H. \end{aligned} \quad (4.22)$$

Note \mathbf{P}_{DDST} is a symmetric matrix such that $\mathbf{U}_D = \mathbf{V}_D$. The last singular value $\dot{\sigma}_{Q-1,Q-1}^D$ is equal to zero, it means the rank of \mathbf{P}_{DDST} is $Q-1$ and the basis of $\mathbf{N}(\mathbf{P}_{\text{DDST}})$ is \mathbf{v}_{Q-1}^D . It can be expressed as

$$\mathbf{N}(\mathbf{P}_{\text{DDST}}) = \text{Span}\{\mathbf{v}_{Q-1}^D\}. \quad (4.23)$$

Furthermore, \mathbf{v}_{Q-1}^D is calculated by SVD method

$$\mathbf{v}_{Q-1}^D = [1, 1, \dots, 1]_{1 \times Q}^T. \quad (4.24)$$

It can be obviously expected since sum of all rows of \mathbf{I}_Q , i.e., $\mathbf{\Theta} = \mathbf{P}_{\text{DDST}} \mathbf{E}$, $\mathbf{E} = \mathbf{I}$, is equal to \mathbf{v}_{Q-1}^D . In proposed precoding scheme, finding a basis of $\mathbf{N}(\mathbf{\Theta})$ by means of SVD method can be simplified. Assume the size of $\mathbf{\Theta}$ is $Q \times Q$, can be decomposed as

$$\mathbf{\Theta} = \mathbf{U}_\theta \mathbf{\Sigma}_\theta \mathbf{V}_\theta^H, \quad (4.25)$$

where $\mathbf{U}_\theta = [\mathbf{u}_0^\theta, \dots, \mathbf{u}_{Q-1}^\theta]$, $\mathbf{V}_\theta = [\mathbf{v}_0^\theta, \dots, \mathbf{v}_{Q-1}^\theta]$. Since $\mathbf{N}(\mathbf{\Theta})$ associates with \mathbf{V}_θ ,

which can be calculated from

$$\begin{aligned} \mathbf{\Theta}^H \mathbf{\Theta} &= \mathbf{V}_\theta \mathbf{\Sigma}_\theta^H \mathbf{U}_\theta^H \mathbf{U}_\theta \mathbf{\Sigma}_\theta \mathbf{V}_\theta^H \\ &= \mathbf{V}_\theta \mathbf{D}_\theta \mathbf{V}_\theta^H, \end{aligned} \quad (4.26)$$

where $\mathbf{D}_\theta = \mathbf{\Sigma}_\theta^H \mathbf{\Sigma}_\theta$ is a diagonal matrix. Substitute Eq. (4.18) into Eq. (4.26), $\mathbf{\Theta}^H \mathbf{\Theta}$

can be expressed as

$$\begin{aligned} \mathbf{\Theta}^H \mathbf{\Theta} &= \mathbf{E}^H \mathbf{P}_{\text{DDST}}^H \mathbf{P}_{\text{DDST}} \mathbf{E} \\ &= \mathbf{E}^H \mathbf{P}_{\text{DDST}} \mathbf{P}_{\text{DDST}} \mathbf{E} \\ &= \mathbf{E}^H \mathbf{P}_{\text{DDST}} \mathbf{E}. \end{aligned} \quad (4.27)$$

According to Eq. (4.22), the above equation can be rewritten as

$$\begin{aligned} \mathbf{\Theta}^H \mathbf{\Theta} &= \mathbf{E}^H \mathbf{U}_D \mathbf{\Sigma}_D \mathbf{V}_D^H \mathbf{E} \\ &= (\mathbf{E}^H \mathbf{V}_D) \mathbf{\Sigma}_D (\mathbf{E}^H \mathbf{V}_D)^H. \end{aligned} \quad (4.28)$$

Comparing Eq. (4.26) with Eq. (4.28), we obtain

$$\mathbf{D}_\theta = \boldsymbol{\Sigma}_D, \mathbf{V}_\theta = \mathbf{E}^H \mathbf{V}_D. \quad (4.29)$$

It means the singular value of $\boldsymbol{\Theta}$ is similar to \mathbf{P}_{DDST} , and all column vectors of $\mathbf{E}^H \mathbf{V}_D$ are right singular vectors of $\boldsymbol{\Theta}$. Note that $(\mathbf{D}_\theta)_{Q-1, Q-1} = \sigma_{Q-1, Q-1}^D = 0$ and the basis of $\mathbf{N}(\boldsymbol{\Theta})$ is \mathbf{v}_{Q-1}^0 . Due to \mathbf{v}_{Q-1}^D was given in Eq. (4.24), every entry in \mathbf{v}_{Q-1}^0 can be obtain as

$$v_{i, Q-1}^0 = \sum_{j=0}^{Q-1} [\mathbf{E}^H]_{i, j}, \quad i = 0, 1, \dots, Q-1, \quad (4.30)$$

where $\mathbf{v}_{Q-1}^0 = [v_{0, Q-1}^0, v_{1, Q-1}^0, \dots, v_{Q-1, Q-1}^0]^T$. Since the basis of $\mathbf{N}(\boldsymbol{\Theta})$ is sum of all rows of \mathbf{E}^H , the forth condition is

$$\text{(C4)} \quad \mathbf{z}'_{i, k} \notin \sum_{j=0}^{Q-1} [\mathbf{E}^H]_{i, j}. \quad (4.31)$$

The above conditions limited the search base of precoding matrix. In next section we will try to find out an appropriate precoding matrix.

4.2 Real or Complex Precoding Matrix

At first, real matrix is not approximate to precode is proved in this section. If a signal $x[n]$ is real and

$$x[n] \begin{matrix} \xrightarrow{\text{FFT}} \\ \xleftarrow{\text{IFFT}} \end{matrix} X[k], \quad 0 \leq n, k \leq Q-1, \quad (4.32)$$

according to the symmetry properties of the DFT [33], the following properties should be hold

$$\begin{cases} |X[k]| = |X[((-k))_N]| \\ \angle\{X[k]\} = -\angle\{X[((-k))_N]\}. \end{cases} \quad (4.33)$$

Assume \mathbf{E}^r is a real matrix which size is Q , the precoding matrix can be shown as

$$\mathbf{\Theta}^r = \mathbf{P}_{\text{DDST}} \mathbf{E}^r, \quad (4.34)$$

and the q -th column of \mathbf{E}^r is given as

$$\mathbf{E}_q^r = [x_{0,q}^r \quad x_{1,q}^r \quad \cdots \quad x_{Q-1,q}^r]^T. \quad (4.35)$$

To satisfy the requirement of Eq. (4.33), signal in frequency domain should be

$$\mathbf{X}_q^r = [a_{0,q} \quad a_{1,q} e^{j\theta_{1,q}} \quad \cdots \quad a_{Q/2-1,q} e^{j\theta_{Q/2-1,q}} \quad a_{Q/2,q} \quad a_{Q/2-1,q} e^{-j\theta_{Q/2-1,q}} \quad \cdots \quad a_{1,q} e^{-j\theta_{1,q}}]^T, \quad (4.36)$$

where $a_{0,q}, a_{1,q}, \cdots, a_{Q/2,q}$ are real numbers, and $\theta_{1,q}, \cdots, \theta_{Q/2-1,q}, \theta_{Q/2+1,q}, \cdots, \theta_{Q-1,q}$ are corresponding phase. According to condition 1, every column of \mathbf{E}^r should have equal amplitude in frequency domain. It means the constraint of full frequency diversity is

$$|a_{0,q}| = |a_{1,q}| = \cdots = |a_{Q/2,q}|. \quad (4.37)$$

Real precoding matrix \mathbf{E}^r can be expressed as

$$\mathbf{E}^r = \mathbf{F}^H \begin{bmatrix} \mathbf{X}_0^r & \mathbf{X}_1^r & \cdots & \mathbf{X}_{Q-1}^r \end{bmatrix}. \quad (4.38)$$

In condition 2, the basis of $\mathcal{N}(\Theta^r)$ is the last column of \mathbf{v}^r

$$\mathbf{v}_{Q-1}^r = \begin{bmatrix} v_{0,Q-1}^r & v_{1,Q-1}^r & \cdots & v_{Q-1,Q-1}^r \end{bmatrix}^T, \quad (4.39)$$

where $v_{s,Q-1}^r$ is the s th element of \mathbf{v}_{Q-1}^r for $s = 0, 1, \dots, Q-1$. It can be expressed as

$$v_{s,Q-1}^r = \sum_{j=0}^{Q-1} \left[(\mathbf{E}^r)^H \right]_{s,j} = \left(\sum_{j=0}^{Q-1} \left[\mathbf{E}^r \right]_{j,s} \right)^T, \quad s = 0, 1, \dots, Q-1. \quad (4.40)$$

Eq. (4.40) holds since \mathbf{E}^r is a real matrix. Substitute Eq. (4.38) to Eq. (4.40), it can be derived as

$$\begin{aligned} v_{s,Q-1}^r &= \left(\sum_{j=0}^{Q-1} \left[\mathbf{F}^H \begin{bmatrix} \mathbf{X}_0^r & \mathbf{X}_1^r & \cdots & \mathbf{X}_{Q-1}^r \end{bmatrix} \right]_{j,s} \right)^T \\ &= \left\{ \left(\sum_{j=0}^{Q-1} \left[\mathbf{F}^H \right]_{j,s} \right) \begin{bmatrix} \mathbf{X}_0^r & \mathbf{X}_1^r & \cdots & \mathbf{X}_{Q-1}^r \end{bmatrix} \right\}^T \\ &= \begin{bmatrix} \mathbf{X}_{0,0}^r & \mathbf{X}_{0,1}^r & \cdots & \mathbf{X}_{0,Q-1}^r \end{bmatrix}^T. \end{aligned} \quad (4.41)$$

Since IDFT operation and sum operation are commutative, it is easy to calculate Eq.

(4.41). Row sum of normalized IDFT matrix is equal to a vector which the first element

is one and the other elements are all zero. The final result is equal to the first element of

\mathbf{X}_q^r , for $q = 0, 1, \dots, Q-1$. Since $a_{0,q}$ is a real number and $|a_{0,0}| = |a_{0,q}| = \cdots = |a_{0,Q-1}|$

for normalized energy, it is easy to prove that it did not satisfy **C4**.

4.3 Proposed Precoding Matrix

In this section, a complex precoding matrix is proposed which satisfies the above mentioned conditions **C1**–**C4**. The DFT and IDFT matrices are popular complex transform matrices, according to [34], we proposed a new precoding matrix that is

$$\mathbf{\Theta}^{\text{ZC}} = \mathbf{P}_{\text{DDST}} \mathbf{E}_{\text{ZC}}, \quad (4.42)$$

where

$$\mathbf{E}_{\text{ZC}} = \frac{1}{\sqrt{Q}} \mathbf{D}_{\text{ZC}} \mathbf{F}^H, \quad (4.43)$$

and \mathbf{F}^H is an IDFT operation. For a low complexity transmitter architecture, \mathbf{D}_{ZC} is chosen to be a diagonal matrix which diagonal elements consist of an arbitrary periodically perfect sequence γ_M . In this work, the Zadoff-Chu sequence is adopted and can be expressed as

$$\gamma_M [n] = \begin{cases} e^{\frac{-j\pi Mn(n+2k)}{Q}}, & n = 0, 1, \dots, Q-1, \text{ for even } Q \\ e^{\frac{-j\pi Mn(n+2k+1)}{Q}}, & n = 0, 1, \dots, Q-1, \text{ for odd } Q. \end{cases} \quad (4.44)$$

Since perfect sequence has equal gain in both the time and frequency domain, the proposed precoding matrix $\mathbf{\Theta}^{\text{ZC}}$ can achieve full frequency diversity. It also satisfies **C1** and separate subgroups independently for **C2**. Moreover, there is no $\mathbf{a}'_{i,k}$ that can be expressed as the linear combination of basis of $\mathbf{N}(\mathbf{\Theta}^{\text{ZC}})$. The test results of each

Table II

Common Matrices

\mathbf{E}_i	C1	C2	C3	C4
$\mathbf{E}_1 = \mathbf{F}^H$	N	Y	Y	N
$\mathbf{E}_2 = \mathbf{P}\mathbf{F}^H$	N	Y	Y	N
$\mathbf{E}_3 = \mathbf{T}\mathbf{F}^H$	N	Y	Y	N
$\mathbf{E}_4 = \mathbf{P}\mathbf{T}\mathbf{F}^H$	N	Y	Y	N
$\mathbf{E}_5 = \mathbf{R}^D\mathbf{F}^H$	N	Y	Y	Y
$\mathbf{E}_6 = \mathbf{R}\mathbf{F}^H$	N	Y	N	Y
$\mathbf{E}_7 = \mathbf{D}^{ZC}\mathbf{F}^H$	Y	Y	Y	Y

Y = condition of \mathbf{E}_i satisfied, N = condition of \mathbf{E}_i not satisfied, \mathbf{P} = permutation matrix, \mathbf{T} = Hadamard matrix, \mathbf{R}^D = diagonal matrix with elements are random phase, \mathbf{R} = a matrix where all elements are random phase.

condition for some well-known matrices are shown in Table II. Finally, a precoding matrix which can satisfy all conditions is proposed.

Chapter 5 Simulation Results

In this section, simulation results demonstrate the performance of the ISSD algorithm [8], ICS algorithm [29] and our proposed method that donate \mathbf{G}^{ZC} . For these schemes, we utilize MMSE equalizer to compensate the channel effect in frequency domain. Notice the performance of channel estimation is not main issue in this work, so we assume perfect channel estimation and synchronization. The selections of the modulation schemes are BPSK and QPSK. The simulations are performed in multipath Rayleigh fading channel with an exponential power decay profile. The CP length is just equal to channel length to avoid IBI and ISI.

Figure 5.2-5.5 show the comparison of BER performance versus signal to noise ratio (SNR) by Monte Carlo simulations with different schemes, ISSD, ICS and our proposed schemes, respectively. In general, we treat the performance of SC-FDE as ideal bound compare with other schemes. For BPSK modulation, the proposed precoding matrix with ISSD is used. In addition, to point up every transmitted subblock is uniquely determined, maximum likelihood (ML) detection is used for high order modulation, and the criterion is

$$\hat{\mathbf{x}}_i = \arg \min_{\mathbf{x} \in \Omega_{ML}} \|\bar{\mathbf{r}}_i - \mathbf{G}^{ZC} \mathbf{x}\|_2.$$

A comparison of the PAPR performance for SC-FDE, DDST and OFDM systems is shown in Fig. 5.1. It is observed that the proposed precoding matrix slightly higher than DDST system for $N=64$, $L=16$. When the space between pilot subcarriers is decreased, the DDST system becomes closer to that of the SC-FDE scheme. Since the frequency components of block has L (L is small) nulls, the DDST system is closed to SC-FDE system and the proposed method approaches to OFDM as shown in Fig 5.2.

Fig. 5.3-5.4 show the BER performance for BPSK modulation with different simulation parameters. The proposed scheme with ISSD is enough to provide good performance for BPSK. When the block size is very larger than channel length, there is a very small probability that transmitted symbols within a subgroup are the same, so the error floor phenomenon occurs at the $BER = (1/2)^{N/L}$.

Fig. 5.5-5.6 display the BER performance for QPSK modulation. It can be seen the performance of proposed method with ML detection is great and has no error floor. On the other hand, ISC does not improve the performance for QPSK. Since the true value of artificial distortion is never more than the decision bound, and always move distorted subgroup to the correct constellation point in first hard decision. So, the ISC method is not much help for QPSK. For high QAM modulation, the ISC method can improve the BER performance, but the error floor still exists.

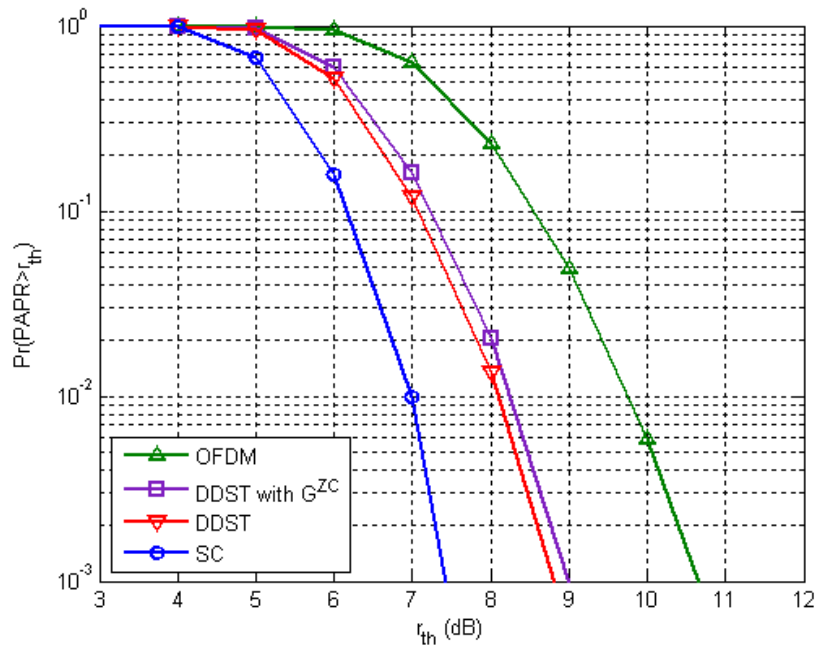


Fig. 5.1. PAPR Performance of different schemes (QPSK, $N=64$, $L=16$).

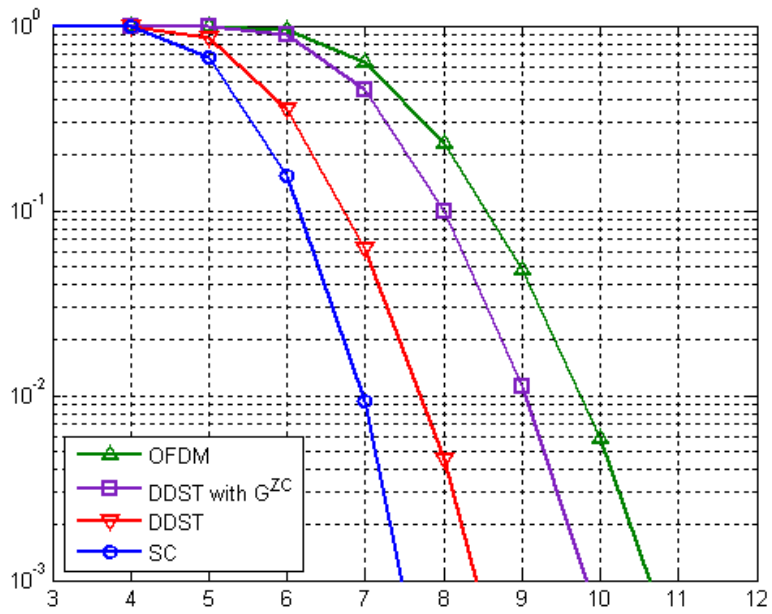


Fig. 5.2. PAPR Performance of different schemes (QPSK, $N=64$, $L=8$).

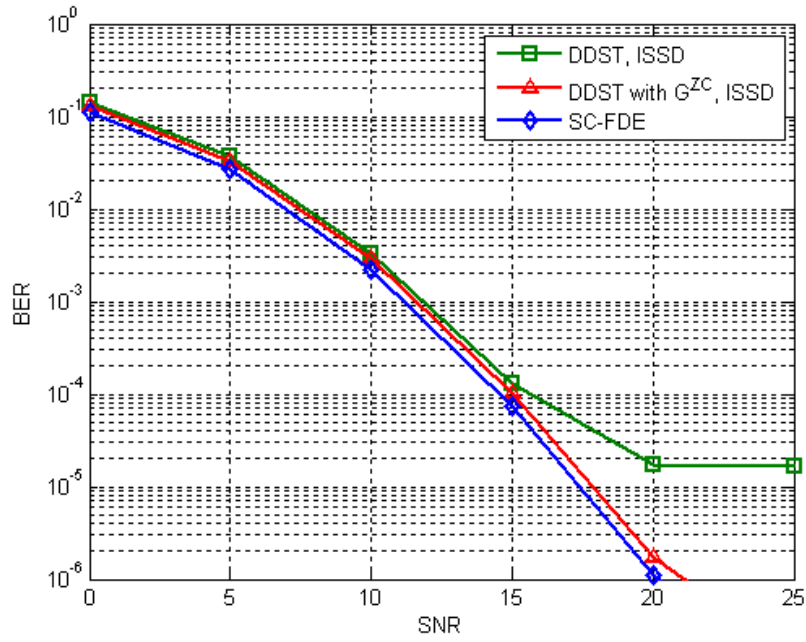


Fig. 5.3. Performance comparison of different schemes (BPSK, $N=64$, $L=4$).

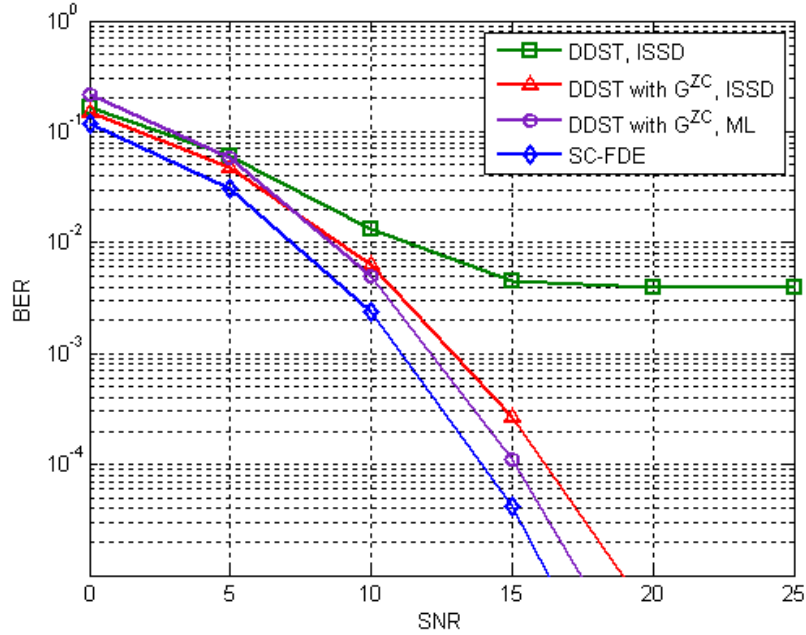


Fig. 5.4. Performance comparison of different schemes (BPSK, $N=64$, $L=8$).

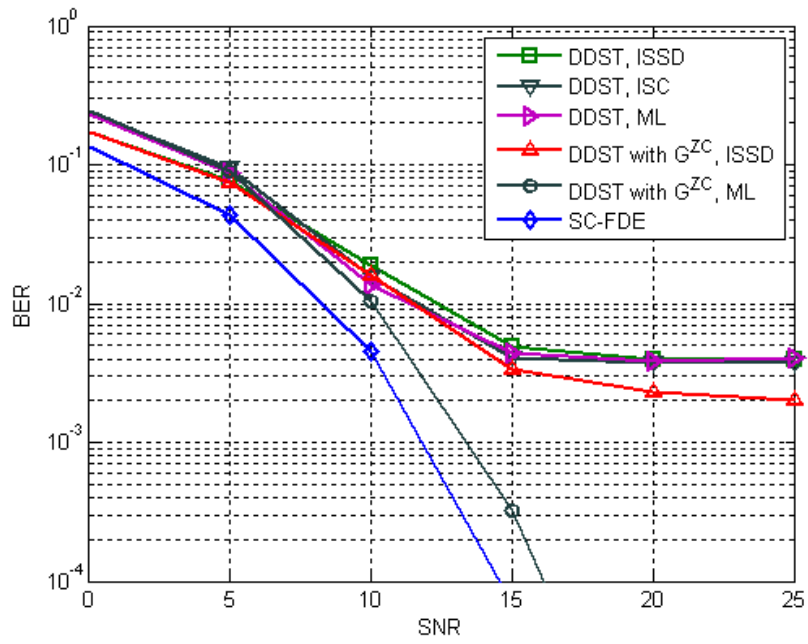


Fig. 5.5. Performance comparison of different schemes (QPSK, $N=256$, $L=32$).

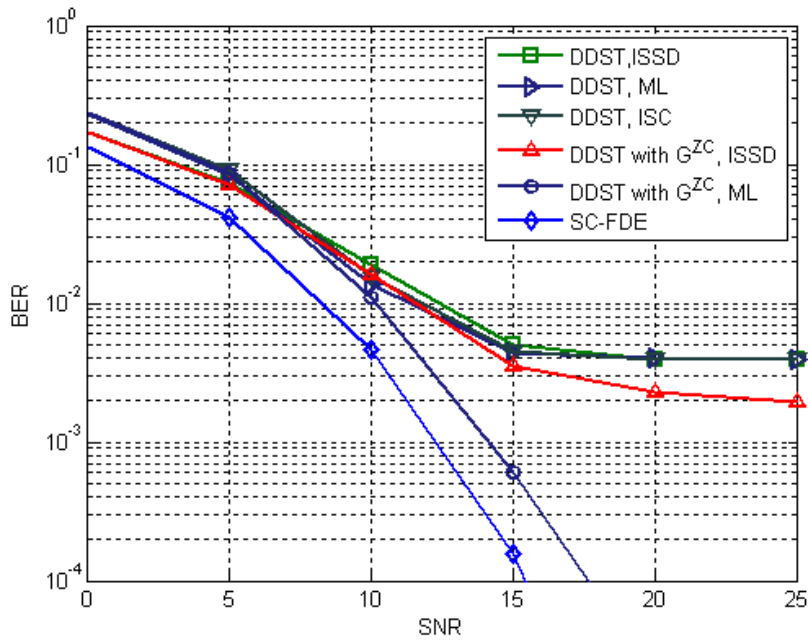


Fig. 5.6. Performance comparison of different schemes (QPSK, $N=64$, $L=8$).

Chapter 6 Conclusion and Future Works

6.1 Conclusions

We analyze the main reasons of data misidentification by SVD method. To overcome this problem, we list some conditions that can help the precoding matrix to enhance BER performance for DDST system. Our proposed method can satisfy these conditions and avoid the precoded subgroup falling into the null space, which impacts that every precoded subgroup is uniquely determined by new method. The simulation results show that the proposed method is feasible and the data identification problem is solved.

6.2 Future Works

This thesis we focus on the data identification problem. When using proposed method with ISSD, it is obviously that the drawback disappears and enough to supply excellence performance for BPSK modulation. For high QAM modulation, it is also can achieve good performance by ML detection, but the computer complexity is very high. How to reduce the complexity of the ML detection for our method is worth researching.

References

- [1] *IEEE Standard for Local and Metropolitan Area Networks*, IEEE Std. 802.16-2004, Oct. 2004.
- [2] *IEEE Draft Standard for Broadband over Power Line Networks:Medium Access Control and Physical Layer Specifications*, IEEE P1901/D3.00, Feb. 2010.
- [3] S. H. Han and J. H. Lee, “An overview of peak-to-average power ratio reduction techniques for multicarrier transmission transmission,” *IEEE Wireless Commun.*, vol. 12, no. 2, pp. 56–65, Apr. 2005.
- [4] S. Ohno and G. B. Giannakis, “Optimal training and redundant precoding for block transmissions with application to wireless OFDM,” *IEEE Trans. Commun.*, vol. 50, no. 12, pp. 2113–2123, Dec. 2002.
- [5] K. Hayashi and H. Sakai, “Interference cancellation schemes for single carrier block transmission with insufficient cyclic prefix,” *EURASIP J. Wireless Commun. Netw.*, vol. 2008, 2008, doi:10.1155/2008/130747, Article ID 130747, 12 pp.
- [6] H. Sari, G. Karam, and I. Jeanclaude, “Transmission techniques for digital terrestrial TV broadcasting,” *IEEE Commun. Mag.*, vol. 33, no. 2, pp. 100–109, Feb. 1995.
- [7] R. Negi and J. Cioffi, “Pilot tone selection for channel estimation in a mobile OFDM system,” *IEEE Trans. Consum. Electron.*, vol. 44, pp. 1122–1128, Aug.

- 1998.
- [8] M. Ghogho, D. McLernon, E. Ananthram-Hernandez, and A. Swami, “Channel estimation and symbol detection for block transmission using data-dependent superimposed training,” *IEEE Signal Process. Lett.*, vol. 12, no. 3, pp. 226–229, Mar. 2005.
- [9] M. Ghogho, T. Whitworth, A. Swami, and D. McLernon, “Full-rank and rank-deficient precoding schemes for single-carrier block transmissions,” *IEEE Trans. Signal Process.*, vol. 57, no. 11, pp. 4433–4442, Nov. 2009.
- [10] F. Wang, J. Tan, and Y. Li, “Precoded single carrier data transmission with orthogonal frequency domain multiplexing pilots,” in *Proc. IEEE ICC*, Beijing, CHN, May 2008, pp. 673–677.
- [11] B. Muquet, M. d. Courville, and P. Duhamel, “Subspace-based blind and semi-blind channel estimation of OFDM systems,” *IEEE Trans. Signal Process.*, vol. 50, no. 7, pp. 1699–1712, July 2002.
- [12] A. Petropulu, R. Zhang, and R. Lin, “Blind OFDM channel estimation through simple linear precoding,” *IEEE Trans. Wireless Commun.*, vol. 3, no. 2, pp. 647–655, Mar. 2004.
- [13] D. McLernon, E. Alameda-Hernandez, and A. G. Orozco-Lugo, “Implicitly-trained channel estimation and equalization with zero mean input data packets,” in

Proc. IEEE ISSPIT, Rome, ITA, Dec. 2004, pp. 136–139.

- [14] A. G. Orozco-Lugo, M. M. Lara, and D. C. McLernon, “Channel estimation using implicit training,” *IEEE Trans. Signal Process.*, vol. 52, no. 1, pp. 240–254, Jan. 2004.
- [15] L. Deneire, B. Gyselinckx, and M. Engels, “Training sequence versus cyclic prefix—a new look on signal carrier communication,” *IEEE Commun. Letters*, vol. 5, no. 7, pp. 292–294, July 2001.
- [16] S. B. Slimane, “Reducing the peak-to-average power ratio of OFDM signals through precoding,” *IEEE Trans. Veh. Technol.*, vol. 56, no. 2, pp. 686–695, Mar. 2007.
- [17] C. D. Chung, “Spectral precoding for constant-envelope OFDM,” *IEEE Trans. Commun.* vol. 58, no. 2, pp. 555–567, Feb. 2010.
- [18] M. Ma, X. Huang, B. Jiao, and Y. J. Guo, “Optimal orthogonal precoding for power leakage suppression in DFT-based systems,” *IEEE Trans. Commun.* vol. 59, no. 3, pp. 844–853, Mar. 2011.
- [19] T. Hwang and Y. (G) Li “A bandwidth efficient block transmission with frequency-domain equalization,” in *Proc. IEEE 6th Circuits and Systems Symposium on Emerging Technologies: Frontiers of Mobile and Wireless Communication*, Shanghai, CHN, vol. 2, June 2004, pp. 433–436.

- [20] K. Takeda, H. Tomeba, and F. Adachi, "Single-carrier transmission with joint Tomlinson-Harashima precoding and frequency-domain equalization," in *Proc. IEEE VTS APWCS*, Daejeon, KOR., Aug. 2006, pp.262 – 266.
- [21] S.M.A. Moosvi, D. C. McLernon, A. G. Orozco-Lugo, M. M. Lara, and M. Ghogho, "Carrier frequency offset estimation using data-dependent superimposed training," *IEEE Signal Process. Lett.*, vol. 12, no. 3, pp. 179 – 181, Mar. 2008.
- [22] J. Lee, T. Hwang, and Y. (G) Li, "Signal detection for EST based modulation in doubly-selective channels," *IEEE Trans. Signal Process.*, vol. 57, no. 48, pp. 3287 – 3291, Aug. 2009.
- [23] T. Hwang and Y. (G) Li, "Optimum filtering for energy-spreading transform-based equalization," *IEEE Trans. Signal Process.*, vol. 55, no. 3, pp. 1182 – 1187, Mar. 2007.
- [24] T. Hwang and Y. (G) Li, "Novel iterative equalization based on energy-spreading transform," *IEEE Trans. Signal Process.*, vol. 54, no. 1, pp. 190 – 203, Jan. 2006.
- [25] W. Wen, M. Xia, and Y.-C. Wu, "Low complexity pre-equalization algorithms for zero-padded block transmission," *IEEE Trans. Wireless Commun.*, vol. 9, no. 8, pp. 2498 – 2504, Aug. 2010.
- [26] K. Takeda, H. Tomeba, and F. Adachi, "Joint Tomlinson-Harashima precoding and frequency-domain equalization for broadband single-carrier transmission," *IEICE*

- Trans. Commun.*, vol. E91-B, no. 1, pp. 258–266, Jan. 2008.
- [27] H. Li, X. Yuan, X. Lin, and L. Ping, “On water-filling precoding for coded single-carrier systems,” *IEEE Commun. Lett.*, vol. 13, no. 1, pp. 34–36, Jan. 2009.
- [28] J. G. Proakis, *Digital Communications*, 4th ed. McGraw-Hill, 2000.
- [29] T. Whitworth, M. Ghogho, and D.C. McLernon, “Data identifiability for data-dependent superimposed training,” in *Proc. IEEE ICC*, Glasgow, UK, June 2007, pp. 2545–2550.
- [30] B. Noble and J. W. Daniel, *Applied Linear Algebra*. 3rd ed. Prentice Hall, 1988.
- [31] D. Forney and V. Eyuboglu, “Combined equalization and coding using precoding,” *IEEE Comm. Mag.*, vol. 29, pp. 24–34, Dec. 1991.
- [32] M. V. Clark, “Adaptive frequency-domain equalization and diversity combining for broadband wireless communications,” *IEEE J. Sel. Areas Commun.*, vol. 16, no. 8, pp. 1385–1395, Oct. 1998.
- [33] A. V. Oppenheim, R. W. Schaffer, and J. R. Buck, *Discrete-Time Signal Processing*. 2nd ed., Prentice Hall, 1999.
- [34] C.-P. Li and W.-C. Huang, “A constructive representation for the Fourier dual of the Zadoff–Chu sequences,” *IEEE Trans. Inf. Theory*, vol. 53, no. 11, pp. 4221–4224, Nov. 2007.

Abbreviations

0-9

3GPP 3rd Generation Partnership Project

A

AWGN Additive White Gaussian Noise

B

BER Bit Error Rate

BPSK Binary Phase Shift Keying

C

CP Cyclic Prefix

CSI Channel State Information

D

DDST Data Dependent Superimposed Training

DFT Discrete Fourier Transform

G

GICS Gradient Infinite Constellation Shift

I

IBI Inter Block Interference

ISI	Inter Symbol Interference
IDFT	Inverse Discrete Fourier Transform
ISSD	Iterative Symbol-by-Symbol Detection
ICS	Infinite Constellation Shift
L	
LTE	Long Term Evolution
LS	Least Square
M	
MSE	Mean Square Error
MMSE	Minimum Mean Square Error
ML	Maximum Likelihood
O	
OFDM	Orthogonal Frequency Division Multiplexing
P	
PLC	Power Line Communication
PAPR	Peak to Average Power Ratio
Q	
QAM	Quadrature Amplitude Modulation
QPSK	Quadrature Phase Shift Keying

S

SVD Singular Value Decomposition

SC-FDE Single Carrier with Frequency Domain equalization

ST Superimposed Training

T

TDM Time Division Multiplexing

W

WiMAX Worldwide Interoperability for Microwave Access

Z

ZF Zero Forcing